THE DISCOVERY BY COMPUTER SIMULATION OF FUNDAMENTAL SINGLE MOLECULE CROSS-CORRELATION FUNCTIONS IN THE LIQUID STATE OF MATTER

M.W. EVANS
Dept. of Physics, U.C.N.W., Bangor, Gwynedd, Wales

Computer simulation and analytical theory are used to characterise, for the first time, the fundamental cross-correlation function (c.c.f.) between a molecule's linear centre of mass velocity ($\boldsymbol{v}$) and its own angular velocity ($\boldsymbol{\omega}$) or angular momentum ($\boldsymbol{J}$) in the laboratory frame of reference.

The c.c.f. $\langle\boldsymbol{v}(t)\boldsymbol{\omega}^{\mathrm{T}}(0)\rangle$ is made visible in the laboratory frame by breaking the overall parity symmetry of the hamiltonian by application of directional force to the molecular ensemble, in this paper a unidirectional, static, external, electric field of force ($\boldsymbol{E}$).

The characteristics of $\langle\boldsymbol{v}(t)\boldsymbol{\omega}^{\mathrm{T}}(0)\rangle$ are investigated for different field strengths $\boldsymbol{E}$ and its appearance is linked analytically to measurable electric-field induced far infra-red birefringence in liquids and liquid crystals.

1. Introduction

The statistical correlation between molecular rotation, measured through the molecular angular velocity ($\boldsymbol{\omega}$) or angular momentum ($\boldsymbol{J}$), and molecular centre of mass translation, measured through the centre of mass linear velocity ($\boldsymbol{v}$), is fundamental to our understanding of the liquid and condensed states of molecular matter. The simplest way to express this statistical relation is through the cross-correlation matrix $\boldsymbol{C}_{\mathrm{tr}} = \langle\boldsymbol{v}(t)\boldsymbol{\omega}^{\mathrm{T}}(0)\rangle$ (or $\langle\boldsymbol{v}(t)\boldsymbol{J}^{\mathrm{T}}(0)\rangle$), the $\boldsymbol{C}_{\mathrm{tr}}$ function. There have been many attempts to describe $\boldsymbol{C}_{\mathrm{tr}}$ analytically in the laboratory frame, starting with the important work of Condiff and Dahler [1], who used the terminology and methods of the Kirkwood school, based on hydrodynamics and the diffusion theory originally due to Einstein.

Many of these papers are, however, incomplete, in that they have attempted to construct theories for $\boldsymbol{C}_{\mathrm{tr}}$ for an isolated molecular ensemble free of any externally applied force field. In this case

$$\boldsymbol{C}_{\mathrm{tr}} = \boldsymbol{0} \quad \text{for all } t, \tag{1}$$

because the sign of $\boldsymbol{v}$ with parity inversion is changed, and that of $\boldsymbol{\omega}$ and $\boldsymbol{J}$ is unaffected. Eq. (1) follows via a theorem due to Berne et al. [2–4], published in final form in 1976.

Berne et al. excluded [3, 4] from the parity veto molecular ensembles to which are applied fields of force, vectors, whose directional properties imply that the complete hamiltonian under consideration is itself changed in response to parity inversion. (In other words if the coordinates and linear momenta all change sign the complete hamiltonian does not remain the same.) This invalidates eqn. (1), and means that $\boldsymbol{C}_{\mathrm{tr}}$ does not necessarily vanish in the presence, for example, of an electric field, $\boldsymbol{E}$, or magnetic field $\boldsymbol{H}$.

It is true that a magnetic field has different parity and time-reversal properties to an electric field, but this does not necessarily deny it the ability of inducing rotation–translation coupling. For example, if the molecule has a magnetic dipole moment $\boldsymbol{\mu}_{\mathrm{m}}$ and is subject to a magnetic field $\boldsymbol{H}$, there is a torque $-\boldsymbol{\mu}_m \times \boldsymbol{H}$ generated analogous to the electric torque to be considered in this paper. It is significant in this context that a magnetic field aligns a nematic liquid crystal, causing a large lab. frame bire-

0378-4363/85/$03.30 © Elsevier Science Publishers B.V.
(North-Holland Physics Publishing Division)

fringence. Birefringence implies the presence of rotation–translation coupling, as this paper aims to show.

This paper reports the discovery of the $\boldsymbol{C}_{\mathrm{tr}}$ function by computer simulation. The characteristics of $\boldsymbol{C}_{\mathrm{tr}}$, produced by computer simulation, are interpreted with simple analytical theory developed by Grigolini et al. [5] for molecular motion in the presence of a static electric field.

An experimental method of measuring $\boldsymbol{C}_{\mathrm{tr}}$ is suggested using electric field induced birefringence [6] in the far infra-red.

2. The algorithm

The search for $\boldsymbol{C}_{\mathrm{tr}}$ was carried out on a model of the C_{2v} molecule dichloromethane chosen for the E.M.L.G. pilot project [7]. The molecule was modelled with a very simple 3 × 3 Lennard-Jones atom–atom potential, taking the $-CH_2$ groups as moieties. Partial charges were made to suffice as a first-order approximation to the electrostatic forces between 108 of these CH_2Cl_2 model potentials. The complete potential is fully described in the literature, together with Ferrario's extensions [8] of the Verlet algorithm used in the numerical integration of Newton's equations for the ensemble. The standard assumptions were made about pair-additivity, boundary conditions and long-range cut-off in the potential. These are also described in more detail elsewhere [8]. The temperature of the runs was 293 K, and the molar volume 10^{-4} m^3 as in ref. 8.

The newly developed technique of field-effect computer simulation was employed to apply to the 108 molecule ensemble an external, static, electric field $\boldsymbol{E}$ in the z-axis of the laboratory frame. This exerts on each molecule a torque

$$\boldsymbol{F} = -\boldsymbol{\mu} \times \boldsymbol{E}, \tag{2}$$

where μ is the molecular (electric) dipole moment. By incorporating $\boldsymbol{F}$ in the forces loop of the algorithm it becomes possible to monitor the transient development of birefringence in the system [7, 9] and after equilibrium, the field-on correlation functions (c.f.'s), including the nine elements of $\boldsymbol{C}_{\mathrm{tr}}$. Each element is normalised, e.g.

$$C_{\mathrm{tr}}^{xy} = \frac{\langle v_x(t)\omega_y(0)\rangle}{\langle v_x^2\rangle^{1/2}\langle \omega_y^2\rangle^{1/2}}, \tag{3}$$

$$C_{\mathrm{tr}}^{yx} = \frac{\langle v_y(t)\omega_x(0)\rangle}{\langle v_y^2\rangle^{1/2}\langle \omega_x^2\rangle^{1/2}}, \tag{4}$$

and so on. At field-on equilibrium, laboratory frame components of normalised autocorrelation functions (a.c.f.'s) ∥ and ⊥ to the electric field are different in time dependence, because the liquid is *birefringent* [6], i.e. no longer isotropic.

The transient regression to equilibrium (after $\boldsymbol{E}$ is removed instantaneously) may also be monitored by computer simulation as orientational fall-transients [9]. Another recent discovery made by simulation is that fall transients are *accelerated* progressively in their time dependence with respect to the equivalent normalised orientational a.c.f. as the external field strength $\boldsymbol{E}$ is increased. This effect, the decay after strong excitation (D.A.S.E.) has a fundamental bearing on the theory of the Brownian motion therefore be described with the classical theory of Debye or Langevin for decoupled rotational or translational diffusion [11]. It is clear that D.A.S.E. is related to the transient process

$$\boldsymbol{C}_{\mathrm{tr}}(\boldsymbol{E} \neq \boldsymbol{0}) \to \boldsymbol{C}_{\mathrm{tr}}(\boldsymbol{E} = \boldsymbol{0}) = \boldsymbol{0}\,.$$

The inter-molecular pair-potential for CH_2Cl_2 was modelled with

$$\varepsilon/k(\mathrm{Cl{-}Cl}) = 173.5\ \mathrm{K};\quad \varepsilon/k(\mathrm{CH_2{-}CH_2}) = 70.5\ \mathrm{K};\quad \sigma(\mathrm{CH_2{-}CH_2}) = 3.96\ \text{Å};\quad \sigma(\mathrm{Cl{-}Cl}) = 3.35\ \text{Å};$$

$$q_{\mathrm{Cl}} = -0.15|e|;\quad q_{\mathrm{CH_2}} = 0.30|e|\,.$$

The noise level in the simulation can be estimated as the difference in $\boldsymbol{C}_{\mathrm{tr}}$ between two successive runs. By symmetry $\boldsymbol{C}_{\mathrm{tr}} = \boldsymbol{0}$ at $t = 0$ for all $\boldsymbol{E}$, so that any departure in the simulation is due to noise. Approximately 1000 records (3000 time steps each of 5×10^{-15} s) were used in constructing $\boldsymbol{C}_{\mathrm{tr}}$ elements. The noise level could be reduced considerably given the computer time, or by repeated averaging. There is no scientific reason for precluding field strengths in the simulation equivalent to the "experimentally accessible" $\mu E/kT \ll 1$. The simulation would simply require more time steps (e.g. 20,000 or 30,000 or more).

The simulation runs were all steady-state runs under a constant electric field. Equilibration was reached under the influence of the field, and the first few thousand time steps rejected as in a normal simulation. There are no abnormal temperature effects with this method.

3. Analytical theory

This is intended to try to understand the numerical results in terms of as few parameters as possible. We therefore use a "bare-bones" theory, starting with the generalised Langevin equation [5]

$$\frac{\mathrm{d}}{\mathrm{d}t}\boldsymbol{C}(t) = \boldsymbol{\lambda}(t)\boldsymbol{C}(t) - \int_0^t \boldsymbol{\phi}(t-\tau)\boldsymbol{C}(\tau)\,\mathrm{d}\tau \tag{5}$$

and the correlation matrix

$$\boldsymbol{C}(t) = \begin{bmatrix} \langle \boldsymbol{v}(t)\boldsymbol{v}^{\mathrm{T}}(0)\rangle & \langle \boldsymbol{v}(t)\boldsymbol{\omega}^{\mathrm{T}}(0)\rangle \\ \langle \boldsymbol{\omega}(t)\boldsymbol{v}^{\mathrm{T}}(0)\rangle & \langle \boldsymbol{\omega}(t)\boldsymbol{\omega}^{\mathrm{T}}(0)\rangle \end{bmatrix} \tag{6}$$

so that the elements of $\boldsymbol{C}(t)$ are correlation functions of $\boldsymbol{v}$ and $\boldsymbol{\omega}$.

In order to reduce the problem to its simplest form, we make the following assumptions:

1) The three molecular moments of inertia are put equal, so that the dynamics of the molecule are those of a "spherical top" with moment of inertia I.

2) It is assumed that the molecule carries a net dipole moment $\boldsymbol{\mu}$, which interacts with an external electric field $\boldsymbol{E}$

For a field $\boldsymbol{E}$ applied in the z-axis of the laboratory frame of reference the computer simulation shows that the matrices $\boldsymbol{C}_{\mathrm{tr}}(t)$ or $\boldsymbol{C}_{\mathrm{rt}}(t)$ may be approximated as

$$\boldsymbol{C}_{\mathrm{tr}}(\mathrm{t}) = \mathbf{C}_{\mathrm{rt}}(t) \div C_{\mathrm{tr}}^{xy}(t)\begin{bmatrix} \delta & -1 & \delta \\ 1 & \delta & \delta \\ \delta & \delta & \delta \end{bmatrix}, \tag{7}$$

i.e. the dominant elements are the (x, y) and (y, x) elements, which are mirror images. In eq. (7) $C_{\mathrm{tr}}^{xy}(t)$ is the scalar c.c.f. obtained by computer simulation.

It is important to note that the electric field has the dual role of promoting the existence of $C_{\mathrm{tr}}(t) = C_{\mathrm{rt}}(t)$ in the laboratory frame and of making the sample anisotropic. This means that

$$\langle v_x^2 \rangle = \langle v_y^2 \rangle \neq \langle v_z^2 \rangle \,, \tag{8}$$

$$\langle \omega_x^2 \rangle = \langle \omega_y^2 \rangle \neq \langle \omega_z^2 \rangle \,. \tag{9}$$

The interaction $-\boldsymbol{\mu} \times \boldsymbol{E}$ appears in eq. (5) through the matrix $\boldsymbol{\lambda}(t)$. We assume that this matrix can be written in the form

$$\boldsymbol{\lambda} = \mathrm{i}\omega_1 \begin{bmatrix} \boldsymbol{0} & \boldsymbol{0} \\ \boldsymbol{0} & \boldsymbol{1} \end{bmatrix} , \tag{10}$$

where $\boldsymbol{0}$ is the null matrix and $\boldsymbol{1}$ the unit matrix, with the scalar frequency

$$\omega_1 = \left(\frac{\mu E_z}{I} \right)^{1/2} .$$

Eq. (10) comes from the fact that the only *direct* influence of $\boldsymbol{E}$ on the molecular motion is the creation of the torque $-\boldsymbol{\mu} \times \boldsymbol{E}$. There is no *direct* influence on the linear centre of mass velocity ($\boldsymbol{v}$), so that terms in $\boldsymbol{\lambda}$ involving $\boldsymbol{v}$ vanish.

Laplace transformation of eq. (1) gives

$$[p\boldsymbol{1} + \boldsymbol{\phi}(p) - \mathrm{i}\omega_1 \boldsymbol{1}] \boldsymbol{C}(p) = \boldsymbol{C}(0) \,. \tag{11}$$

The supermatrices in eq. (11) are defined by

$$\boldsymbol{C}(0) = \begin{bmatrix} \boldsymbol{C}_{\mathrm{tt}}(0) & \boldsymbol{0} \\ \boldsymbol{0} & \boldsymbol{C}_{\mathrm{rr}}(0) \end{bmatrix} ; \quad \boldsymbol{C}(p) = \begin{bmatrix} \boldsymbol{C}_{\mathrm{tt}}(p) & \boldsymbol{C}_{\mathrm{tr}}(p) \\ \boldsymbol{C}_{\mathrm{rt}}(p) & \boldsymbol{C}_{\mathrm{rr}}(p) \end{bmatrix} ,$$

where

$$\boldsymbol{C}_{\mathrm{tt}}(0) = \begin{bmatrix} \langle v_x^2 \rangle & 0 & 0 \\ 0 & \langle v_y^2 \rangle & 0 \\ 0 & 0 & \langle v_z^2 \rangle \end{bmatrix} ; \quad \boldsymbol{C}_{\mathrm{rr}}(0) = \begin{bmatrix} \langle \omega_x^2 \rangle & 0 & 0 \\ 0 & \langle \omega_y^2 \rangle & 0 \\ 0 & 0 & \langle \omega_z^2 \rangle \end{bmatrix} ;$$

$$[(p - \mathrm{i}\omega_i)\boldsymbol{1} + \boldsymbol{\phi}(p)] = \begin{bmatrix} (p - \mathrm{i}\omega_1)\boldsymbol{1} + \boldsymbol{\phi}_{\mathrm{tt}}(p) & \boldsymbol{\phi}_{\mathrm{tr}}(p) \\ \boldsymbol{\phi}_{\mathrm{rt}}(p) & (p - \mathrm{i}\omega_1)\boldsymbol{1} + \boldsymbol{\phi}_{\mathrm{rr}}(p) \end{bmatrix} .$$

The elements of these matrices are themselves matrices defined by

$$\boldsymbol{\phi}_{\mathrm{tr}} = \boldsymbol{\phi}_{\mathrm{rt}} = \phi_{\mathrm{tr}}^{xy}(p) \begin{bmatrix} 0 & -1 & 0 \\ 1 & 0 & 0 \\ 0 & 0 & 0 \end{bmatrix} ; \quad \boldsymbol{\phi}_{\mathrm{tt}} = \begin{bmatrix} \phi_{\mathrm{tt}}^{xx} & 0 & 0 \\ 0 & \phi_{\mathrm{tt}}^{yy} & 0 \\ 0 & 0 & \phi_{\mathrm{tt}}^{zz} \end{bmatrix}$$

and so on.

For an electric field in the z-axis

$$\left.\begin{array}{l}\phi_{tt}^{xx}(p) = \phi_{tt}^{yy}(p) \neq \phi_{tt}^{zz}(p)\\ \phi_{rr}^{xx}(p) = \phi_{rr}^{yy}(p) \neq \phi_{rr}^{zz}(p)\end{array}\right], \tag{12}$$

and similarly for $\boldsymbol{C}_{tt}(p)$ and $\boldsymbol{C}_{rr}(p)$ and the linear and angular velocity autocorrelation matrices. Comparing scalar elements leads to the following physical effects of electric field induced r/t coupling.

1) For a field $\boldsymbol{E}$ in the z-direction both the linear and angular velocity a.c.f.'s become anisotropic in the laboratory frame.

2) For a coupling matrix of the type (7) there is no effect (with this simple theory) of r/t coupling on $C_{tt}^{zz}(p)$ (or $C_{tt}^{xx}(t)$) and $C_{rr}^{zz}(p)$.

3) We obtain the results:

$$\frac{C_{tt}^{xx}(p)}{C_{tt}^{zz}(p)} = \frac{[\langle v_x^2\rangle + \phi_{tr}^{xy}(p)C_{tr}^{xy}(p)]}{(p + \phi_{tt}^{xx}(p))}\,\frac{(p + \phi_{tt}^{zz}(p))}{\langle v_z^2\rangle}, \tag{13}$$

$$\frac{C_{rr}^{xx}(p)}{C_{rr}^{zz}(p)} = \frac{[\langle \omega_x^2\rangle + \phi_{tr}^{xy}(p)C_{tr}^{xy}(p)](p - \mathrm{i}\omega_1 + \phi_{rr}^{zz}(p))}{\langle \omega_z^2\rangle(p - \mathrm{i}\omega_1 + \phi_{rr}^{xx}(p))} \tag{14}$$

If the anisotropy of the liquid is not too pronounced:

$$\phi_{tt}^{zz}(p) \div \phi_{tt}^{xx}(p), \tag{15}$$

$$\phi_{rr}^{zz}(p) \div \phi_{rr}^{xx}(p). \tag{16}$$

If, furthermore, in the Markov approximation[11], we regard the memory function as a constant multiplied by a delta function in time, then

$$\phi_{tr}^{xy}(p) \div \phi_{tr}^{xy} \tag{17}$$

a constant. The approximation inherent in eq. (17) is the Markov approximation. This is too drastic *when rotation and translation are uncorrelated* (i.e. in the absence of birefringence induced by an electric field), because the theory then reduces to Debye's theory of 1913, with all the shortcomings, now well known [7]. In the Debye theory, the linear and angular velocity auto-correlation functions are pure exponentials, that cannot, therefore, fall below the time axis. The Debye theory produces $\boldsymbol{C}_{tr} = \boldsymbol{0}$ for all t and $\boldsymbol{E}$. It then follows from eqs. (13) to (17) that

$$C_{tr}^{xy}(p) \div \frac{\langle \omega_z^2\rangle}{\phi_{tr}^{xy}}\,\frac{C_{rr}^{xx}(p)}{C_{rr}^{zz}(p)} - \frac{\langle \omega_x^2\rangle}{\phi_{tr}^{xy}} \tag{18}$$

$$\div \frac{\langle v_z^2\rangle}{\phi_{tr}^{xy}}\,\frac{C_{tt}^{xx}(p)}{C_{tt}^{zz}(p)} - \frac{\langle v_x^2\rangle}{\phi_{tr}^{xy}}. \tag{19}$$

The angular velocity a.c.f.'s $C_{rr}^{xx}(p)$ can be approximated with rotational velocity a.c.f.'s in the appropriate limit. The latter a.c.f.'s are Fourier transforms of *the far infra-red power* [11] *absorption coefficient*, which can be measured ∥ and ⊥ to the applied electric field. *It is, therefore, possible to observe the C_{tr}^{xy} function experimentally by far infra-red spectroscopy of liquids or liquid crystals treated with external, electric fields.*

4. Calculation of $C_{\mathrm{tr}}^{xy}(t)$

The supermatrix equation (11) also produces the following, rigorous, relation between components. The approximations leading to the relations (18) and (19) have been used only to make these more transparent to the experimentalist, and need not be used at all.

$$\begin{bmatrix} p+\phi_{\mathrm{tt}}^{xx}(p) & -\phi_{\mathrm{tr}}^{xy}(p) \\ \phi_{\mathrm{tr}}^{xy}(p) & p-\mathrm{i}\omega_1+\phi_{\mathrm{rr}}^{xx}(p) \end{bmatrix} \begin{bmatrix} C_{\mathrm{tt}}^{xx}(p) & -C_{\mathrm{tr}}^{xy}(\mathrm{p}) \\ C_{\mathrm{tr}}^{xy}(p) & C_{\mathrm{rr}}^{xx}(p) \end{bmatrix} = \begin{bmatrix} \langle v_x^2\rangle & 0 \\ 0 & \langle \omega_x^2\rangle \end{bmatrix}.$$

This equation leads to the time-domain results:

$$C_{\mathrm{tr}}^{xy}(t) = -\frac{\langle \omega_x^2\rangle \phi_{\mathrm{tr}}^{xy}\,\mathrm{e}^{-at/2}}{(b-a^2/4)^{1/2}} \sin\left(\left(b-\frac{a^2}{4}\right)^{1/2} t\right),$$

where $b=\phi_{\mathrm{tr}}^{xy}+\phi_{\mathrm{tt}}^{xx}\phi_{\mathrm{rr}}^{xx}-\mathrm{i}\omega_1\phi_{\mathrm{tt}}^{xx}$ and $a=\phi_{\mathrm{tt}}^{xx}+\phi_{\mathrm{rr}}^{xx}-\mathrm{i}\omega_1$. Note that both the real and imaginary parts of eq. (21) vanish at $t=0$, as they must by symmetry, because $v_x(0)$ is always orthogonal at $t=0$ to $\omega(0)$.

For a Hamiltonian invariant to parity inversion, it is probable that the off-diagonal elements of C_{tt} are all zero. *In the presence of an electric field*, however, the Hamiltonian is no longer invariant to parity inversion, and it is not easy to use symmetry arguments, to preclude any element of C_{tt} for $t>0$.

At $t=0$, $\langle v_x(t)\omega_y(0)\rangle=0$ simply because v_x is always perpendicular to ω_y for the same molecule at the same instant in time, so that each component of the average $\langle\,\rangle$ is separately zero.

This can be demonstrated by considering a rigid body which rotates about an axis through a point O in the lab. frame with angular speed ω. The *linear* velocity $\boldsymbol{v}$ of a point P of the body with position vector $\boldsymbol{r}$ is given by $\boldsymbol{v}=\boldsymbol{\omega}\times\boldsymbol{r}$, where $\boldsymbol{\omega}$ is the angular velocity, i.e. a vector with magnitude ω whose direction is that in which a right-handed screw would advance under the given rotation. Since P travels in a circle of radius $r\sin\theta$, the magnitude of the linear velocity $\boldsymbol{v}$ is $\omega(r\sin\theta)=|\boldsymbol{\omega}\times\boldsymbol{r}|$. It follows that $\boldsymbol{v}$ must be perpendicular to both $\boldsymbol{\omega}$ and $\boldsymbol{r}$ at the same instant in time (i.e. $t=0$). Since the linear velocity of the centre of mass can always be made to have the same magnitude and direction as that of the arbitrary point $\boldsymbol{r}$ (by setting $\boldsymbol{r}=\boldsymbol{0}$), it follows that $v(0)\boldsymbol{\omega}^{\mathrm{T}}(0)=\boldsymbol{0}$ for every molecule. Similarly:

$$C_{\mathrm{tt}}^{xx}(t)=\langle v_x^2\rangle\,\mathrm{e}^{-at/2}\left(\cos\left(\left(b-\frac{a^2}{4}\right)^{1/2}t\right)+\frac{(\phi_{\mathrm{tt}}^{xx}-a/2)}{(b-a^2/4)^{1/2}}\sin\left(\left(b-\frac{a^2}{4}\right)^{1/2}t\right)\right),$$

$$C_{\mathrm{rr}}^{xx}(t)=\langle \omega_x^2\rangle\,\mathrm{e}^{-at/2}\left(\cos\left(\left(b-\frac{a^2}{4}\right)^{1/2}t\right)+\frac{(\phi_{\mathrm{rr}}^{xx}-\mathrm{i}\omega_1-a/2)}{(b-a^2/4)^{1/2}}\sin\left(\left(b-\frac{a^2}{4}\right)^{1/2}t\right)\right).$$

Note that when $\omega_1=0$ the equations (22) and (23) decouple into rotational and translational components. Using the identity:

$$\sin(a+\mathrm{i}b)=\sin a\cosh b+\mathrm{i}\cos a\sinh b$$

and the N.A.G. routines A01AAA and A01ACA to evaluate the real part of eqs. (21) to (23), the theory can be applied to the C_{tr} function obtained by computer simulation.

5. Results and discussion

The $\boldsymbol{C}_{\mathrm{tr}}$ function from the computer simulation is illustrated in fig. 1 for various $\mu E/kT$. The (x, y) and (y, x) elements dominate over the others in amplitude for an electric field in the z-axis of the laboratory frame. These can therefore be labelled, for convenience, as the "dominant elements" of the C_{tr} function, i.e. C_{tr}^{xy} and C_{tr}^{yx}. The simulations show that these two elements are *mirror images* within the noise of two successive computer runs. The other seven elements cannot be picked up from the noise, but *may exist.* They could be detected using a super-computer such as Cray IS or Cyber 205 with long runs.

The dominance of C_{tr}^{xy} and C_{tr}^{yx} can be understood simply in terms of the torque $-\boldsymbol{\mu} \times \boldsymbol{E}$ when $\boldsymbol{E}$ is in the z-axis. In vector terms this is

$$(\boldsymbol{i}\mu_y - \boldsymbol{j}\mu_x)E_z$$

where $\boldsymbol{i}$ and $\boldsymbol{j}$ are unit vectors in the x and y axes and μ_y and μ_x components of the dipole moment $\boldsymbol{\mu}$. The torque is basically the same in nature when polarisability effects are introduced, so that little or no new physical insight is gained in this particular context.

The C_{tr}^{xy} (or C_{tr}^{yx}) function is oscillatory, and attains a maximum normalised amplitude (measured by that of the first peak) for *intermediate* field strengths. The other elements of $\boldsymbol{C}_{\mathrm{tr}}$ lie below the noise of the current simulation runs. As the field strength is increased the Grigolini decoupling effect is observed in C_{tr}^{xy} and C_{tr}^{yx}. This means that the external electric field competes with the thermal forces in the molecular ensemble, whose influence on the $\boldsymbol{C}_{\mathrm{tr}}$ function decreases with respect to that of the electric field as the strength of the latter is increased. In consequence, the $\boldsymbol{C}_{\mathrm{tr}}$ function becomes longer lived, as measured through the *envelope* of its oscillations.

At $\mu E/kT = 0.28$ for as few as 3000 time steps C_{tr}^{xy} and C_{tr}^{yx} are still just visible above the noise of

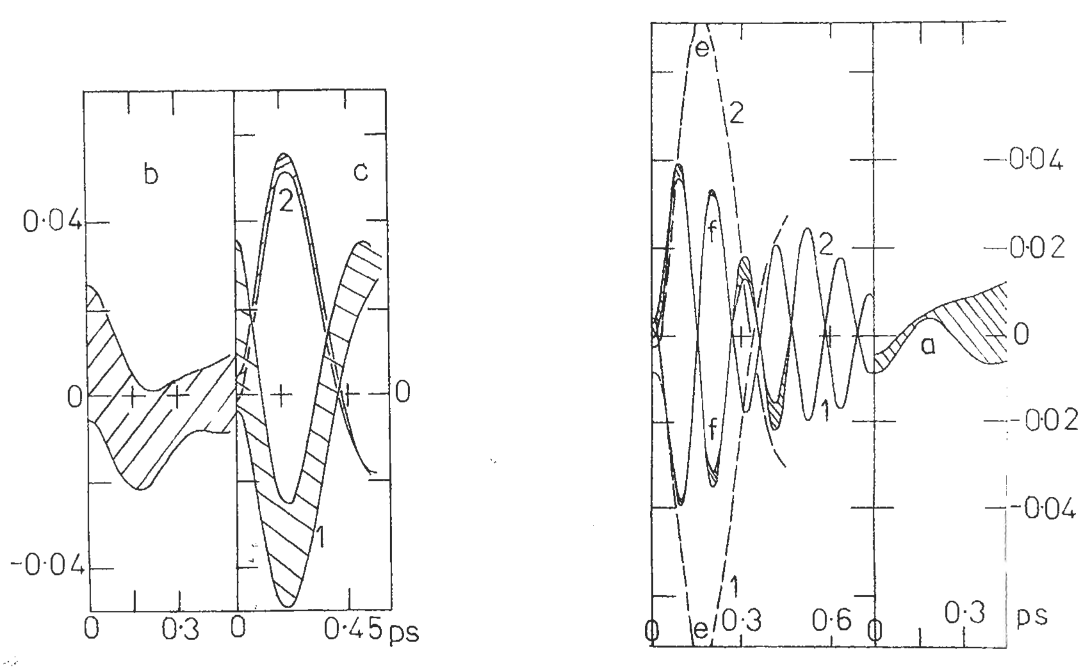

Fig. 1. Development of 1) C_{tr}^{xy} and 2) C_{tr}^{xy} with interaction energy $\mu E/kT$. a) $\mu E/kT = 0.0$ (noise only); b) 0.28 (curve 1 only); c) 1.40; e) 28.0; f) 2.8. *Ordinate*: Normalized c.c.f.; *abscissa*: time/ps.

the simulation. *By using a great deal more computer time the C_{tr} function can be characterised clearly for the experimentally accessible $\mu E/kT \leqslant 0.01$ the condition under which induced-birefringence experiments are usually carried out* [6].

Eq. (21) is illustrated in fig. 2 with a set of test parameters, keeping the ratio ω_1/ϕ_{tr}^{xy} constant. The following points emerge from this illustration:

1) The *envelope* of the oscillations, marked with dashed lines in figs. 2a and 2b, remains constant for constant ω_1/ϕ_{tr}^{xy}.

2) It is possible to observe the function C_{tr}^{xy} even for values of ϕ_{tr}^{xy} *much smaller than* ϕ_{tr}^{xx} or ϕ_{tr}^{zz}.

3) $C_{tr}^{xy}(t)$ from eq. (21) vanishes, as it should, at $t = 0$ and $t \to \infty$.

At intermediate t the normalised amplitude is similar to that from the computer (see fig. 3), but differs in that the initial slope at $t \to 0$ is not zero, because the "bare-bones" theory behind eq. (21) is Markovian in statistical make-up. Unlike the simulated C_{tr} function, the amplitude from eq. (21) decreases monotonically with decreasing field strength. (Recall that the simulated C_{tr} goes through an amplitude maximum at *intermediate* field strengths.) This is another consequence of Markovian statistics in eq. (21)–(23). In consequence, these *cannot* show the Grigolini decoupling effect. The latter is the signature of the non-Markovian statistical properties of molecular dynamics [12].

By symmetry, ϕ_{tr}^{xy} must disappear when $\omega_1 = 0$ (i.e. $\boldsymbol{E} = \boldsymbol{0}$). A theory with more flesh on it than the "bare-bones" (21) to (23) would provide us with this link.

In fig. 3, we compare the analytical and simulated $C_{tr}^{xy}(t)$ and $C_{tr}^{yx}(t)$ c.c.f.'s at 2.8 kT by fitting the simulated $C_{\omega\omega}^{zz}(t)$ function, giving $\phi_{rr}^{zz} = 6.4$ THz; $\omega_1 = 6.0$ THz. For simplicity, it was then assumed that $\phi_{rr}^{zz} \doteqdot \phi_{rr}^{xx} \doteqdot \phi_{tt}^{zz} \doteqdot \phi_{tt}^{xx}$ and the other curves in this figure were generated by varying ϕ_{tr}^{xy} only. Fig. 3 is for $\phi_{tr}^{xy} = 9.0$ THz. *Both* the analytical *and* numerical C_{tr} functions in fig. 3 are therefore derived self-consistently. For these parameters the analytical C_{tr} elements are greater in normalised intensity than the simulated ones, and less oscillatory. The *birefringence* in the simulated and analytical angular velocity a.c.f.'s (eq. (23)) in fig. 3 is in the same sense, but this time the analytical result is the smaller in magnitude for the same parameters as in the C_{tr} comparison. Finally there is a small, but real birefringence in the simulated and analytical (eq. (22)) *linear* velocity a.c.f.'s (fig. 3) which must, of course, come from r/t coupling.

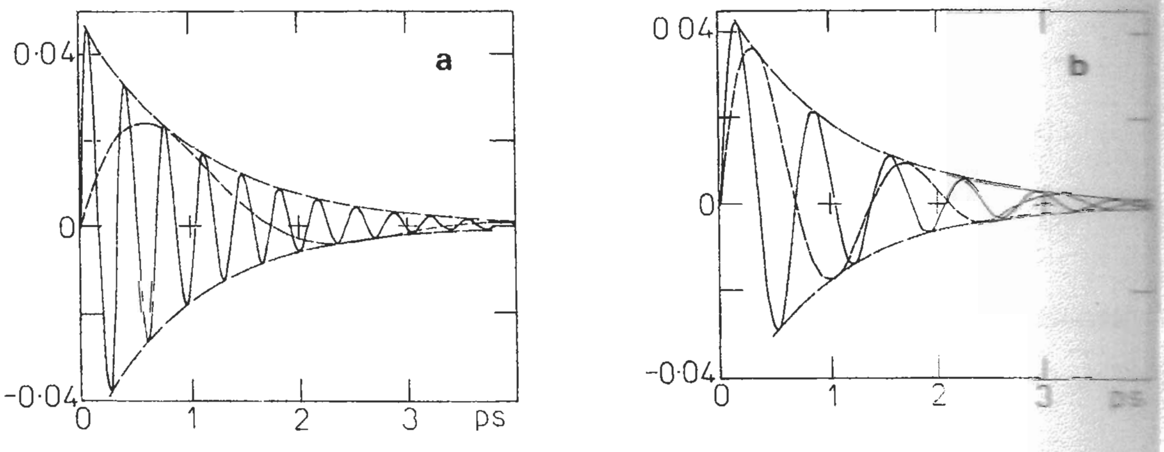

Fig. 2. a) The function $C_{tr}^{yx}/\langle\omega_x^2\rangle$, test parameters $\phi_{tt}^{xx} = \phi_{rr}^{xx} = 10^{12}\ \mathrm{s}^{-1}$; ——— $\phi_{tr}^{xy} = 0.9 \times 10^{12}\ \mathrm{s}^{-1}$; $\omega_1 = 18.0 \times 10^{12}\ \mathrm{s}^{-1}$; ——— $\phi_{tr}^{xy} = 0.09 \times 10^{12}\ \mathrm{s}^{-1}$; $\omega_1 = 1.8 \times 10^{12}\ \mathrm{s}^{-1}$; - - - - - - the oscillation envelope. b) ——— $\phi_{tt}^{xx} = \phi_{rr}^{xx} = 10^{12}\ \mathrm{s}^{-1}$, $\phi_{tr}^{xy} =$ [illegible] 9.0 × $10^{12}\ \mathrm{s}^{-1}$; ——— $\phi_{tr}^{xy} = 0.225 \times 10^{12}\ \mathrm{s}^{-1}$, $\omega_1 = 0.45 \times 10^{12}\ \mathrm{s}^{-1}$. *Ordinate*: $C_{tr}^{xy}/\langle\omega_x^2\rangle$; *abscissa*: time/ps.

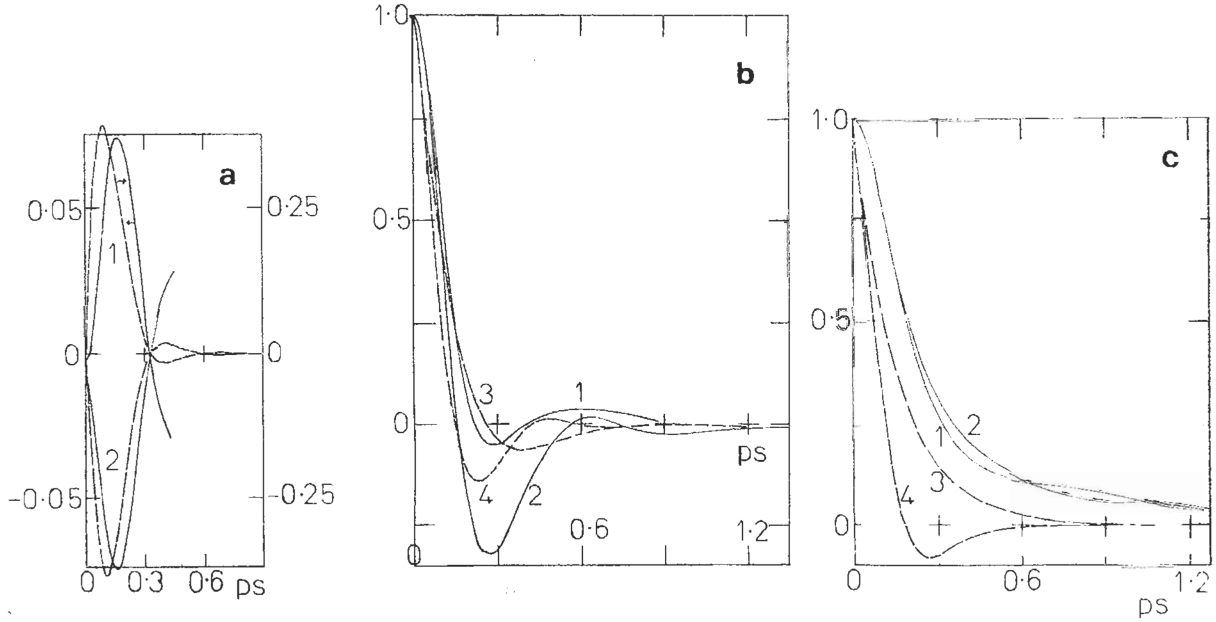

Fig. 3. (a) Simulated and analytical $C_{\mathrm{tr}}^{xy}(t)$ and $C_{\mathrm{tr}}^{yx}(t)$. ——— (1) $C_{\mathrm{tr}}^{xy}(t)$, simulated; ----- analytical theory (R.H. scale). *Ordinate*: Normalised c.c.f.; *abscissa*: time/ps; (b) (1) $\langle\omega_z(t)\omega_z(0)\rangle/\langle\omega_z^2\rangle$; (2) $\langle\omega_x(t)\omega_x(0)\rangle/\langle\omega_x^2\rangle$, the simulated angular velocity a.c.f. $/\!/$ and $\perp$ to the electric field. ----- (3) and (4); as for (1) and (2), respectively, analytical theory. *Ordinate*. normalised a.c.f.; *abscissa*: time/ps. (c) As for fig. 3a; linear, centre of mass, velocity a.c.f.'s.

6. Suggested methods for the experimental observation of the C_{tr} function

1) Rise and fall transients calculated from eq. (5) could be compared with their equivalents from the new electro-optic methods using sub-picosecond laser pulses to induce birefringence.

2) Eq. (18) (or a more rigorous version) can be implemented by looking at electric field induced birefringence in the far infra-red at as many different frequency points as possible. An extremely sensitive method of detecting very low levels of birefringence is via *the rotation of the plane of polarisation of a probe laser* [6]. This method can be used with polarised *carcinotrons or submillimetre lasers* in the far infra-red and with polarised *microwave guides* at lower frequencies. The refractive index at a given frequency could be measured $/\!/$ and $\perp$ to the applied electric field. The resulting birefringence $\Delta n(v)$ could then be converted into power absorption $\Delta\alpha(\bar{v})$ using the Kramers–Kronig relations. Repetition of the experiment at different spot frequencies would provide the required far infra-red power absorption profile $/\!/$ and $\perp$ to $\boldsymbol{E}$. These profiles would be Fourier transformed for subsequent use in eq. (18) as discussed already in this paper.

It is true that the rotational velocity and angular velocity auto-correlation functions are not the same, but under well-known conditions (e.g. relatively high density and relatively low temperature) they become very similar, and therefore the angular velocity correlation-function is well approximated by the Fourier transform of a far infra-red profile. For further remarks in this context see ref. 7 and its companion volume "Molecular Dynamics", ref. 11.

3) Method (2), suitable for normally isotropic liquids such as dichloromethane, becomes feasible with an ordinary Fourier transform interferometer by using *nematic liquid crystals* as samples. The far infra-red spectra $\perp$ and $/\!/$ to a low strength z-axis electric field will be significantly different, and measurable straightforwardly in order to extract the C_{tr} function.

Acknowledgements

The University of Wales is thanked for a Fellowship and the Nuffield Foundation for bursaries. The referee for this paper is thanked for a detailed and worthwhile review, with several constructive comments, incorporated in the text by the author.

References

[1] D.W. Condiff and J.S. Dahler, J. Chem. Phys. 44 (1966) 3988.
[2] G.D. Harpe and B.J. Berne, Phys. Rev. 2 (1970) 975.
[3] N.K. Ailawadi, B.J. Berne and D. Forster, Phys. Rev. A 3 (1971) 1462.
[4] B.J. Berne and R. Pecora, Dynamic Light Scattering with Applications to Physics, Chemistry and Biology (Wiley-Interscience, New York, 1976).
[5] M.W. Evans, P. Grigolini and F. Marchesoni, Chem. Phys. Letters 95 (1983) 544.
[6] M.S. Beevers and D.A. Elliott, Mol. Cryst., Liq. Cryst. 26 (1979) 411.
[7] W.T. Coffey, M.W. Evans and P. Grigolini, Molecular Diffusion and Spectra (Wiley-Interscience. New York, 1984).
[8] M. Ferrario and M.W. Evans, Chem. Phys. 72 (1982) 141, 147.
[9] M.W. Evans, J. Chem. Phys. 76 (1982) 5473, 5480; 77 (1982) 4632; 78 (1983) 925, 5403; J. Mol. Liq. 26 (1983) [illegible].
[10] C.J. Reid, Mol. Phys. 49 (1983) 331.
[11] M.W. Evans, G.J. Evans, W.T. Coffey and P. Grigolini, Molecular Dynamics and Theory of Broad Band Spectroscopy (Wiley-Interscience, New York, 1982).
[12] Memory Function Approach to Stochastic Problems in Condensed Matter, M.W. Evans, P. Grigolini and G. Pastori Parravicini, eds. Chapter I, by P. Grigolini, special issue of Adv. Chem. Phys. series, Vols. 62 and 63 (Wiley-Interscience, New York, 1985).